PNAS
www.pnas.org

Supplementary Information for

The Arabidopsis GRAS-type SCL28 transcription factor controls the mitotic cell cycle and division plane orientation

Camila Goldy, José-Antonio Pedroza-García, Natalie Breakfield, Toon Cools, Rodrigo Vena, Philip N. Benfey, Lieven De Veylder, Javier Palatnik, Ramiro E. Rodriguez

Corresponding author: Ramiro E. Rodriguez (email: rrodriguez@ibr-conicet.gov.ar)

This PDF file includes:
Figures S1 to S9
Tables S1 to S3

Other supplementary materials for this manuscript include the following:
Datasets S1 to S5

Supplementary Figures

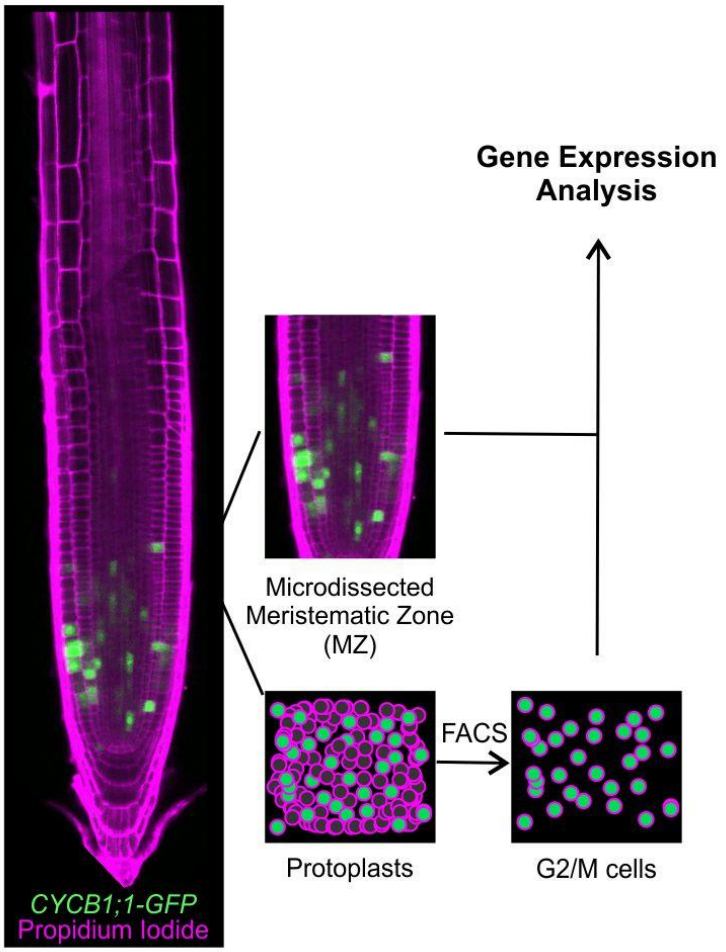

Figure S1. Squematic representation of the metodology used for the analysis of the transcriptome of cells in G2/M.
In the left, a LSCM image of the *CYCB1;1-GFP* reporter (fluorescence in green) in 6-day-old wild-type and *scl28-3* roots stained with propidium iodide (PI, fluorescence in magenta).

GO Term	Description	Genes Enriched in G2/M cells (-LOG10(FDR))	Genes Depleted in G2/M cells (-LOG10(FDR))
GO:0007017	microtubule-based process	6.46	
GO:0006396	RNA processing	4.15	
GO:0007018	microtubule-based movement	3.89	
GO:0034660	ncRNA metabolic process	3.66	
GO:0016072	rRNA metabolic process	3.41	
GO:0000087	M phase of mitotic cell cycle	2.85	
GO:0000910	cytokinesis	1.80	
GO:0048229	gametophyte development	1.77	
GO:0006839	mitochondrial transport	1.49	
GO:0034641	cellular nitrogen compound metabolic process	1.49	
GO:0042542	response to hydrogen peroxide	1.44	
GO:0007049	cell cycle	14.43	2.15
GO:0006807	nitrogen compound metabolic process	4.42	3.05
GO:0009987	cellular process	3.96	1.32
GO:0006139	nucleobase, nucleoside, nucleotide and nucleic acid metabolic process	3.57	3.72
GO:0044085	cellular component biogenesis	2.09	1.36
GO:0051301	cell division	1.89	2.05
GO:0006259	DNA metabolic process	1.49	12.22
GO:0048509	regulation of meristem development		1.32
GO:0009059	macromolecule biosynthetic process		1.33
GO:0007167	enzyme linked receptor protein signaling pathway		1.41
GO:0010556	regulation of macromolecule biosynthetic process		1.44
GO:0044238	primary metabolic process		1.46
GO:0050896	response to stimulus		1.49
GO:0048364	root development		1.49
GO:0008152	metabolic process		1.49
GO:0009725	response to hormone stimulus		1.49
GO:0040007	growth		1.51
GO:0048580	regulation of post-embryonic development		1.60
GO:0048589	developmental growth		1.60
GO:0042545	cell wall modification		1.60
GO:0009719	response to endogenous stimulus		1.60
GO:0010218	response to far red light		1.64
GO:0009058	biosynthetic process		1.72
GO:0006974	response to DNA damage stimulus		1.80
GO:0032502	developmental process		2.41
GO:0032501	multicellular organismal process		3.02
GO:0065007	biological regulation		4.43
GO:0006323	DNA packaging		9.92
GO:0006260	DNA replication		19.09

Figure S2. GO-term enrichment analysis in the lists of genes enriched or depleted in G2/M cells.
GO-term enrichment analysis was performed using the list of genes expressed preferentially in the root meristem and enriched or depleted in G2/M cells. The -LOG10(FDR) is informed when the False Discovery Rate was less than the 0.01 threshold selected for significantly enriched GO-terms. Terms related to cell proliferation are highlighted in blue, while terms related to processes specific to mitosis and cytokinesis or S-phase are highlighted in green or red, respectively.

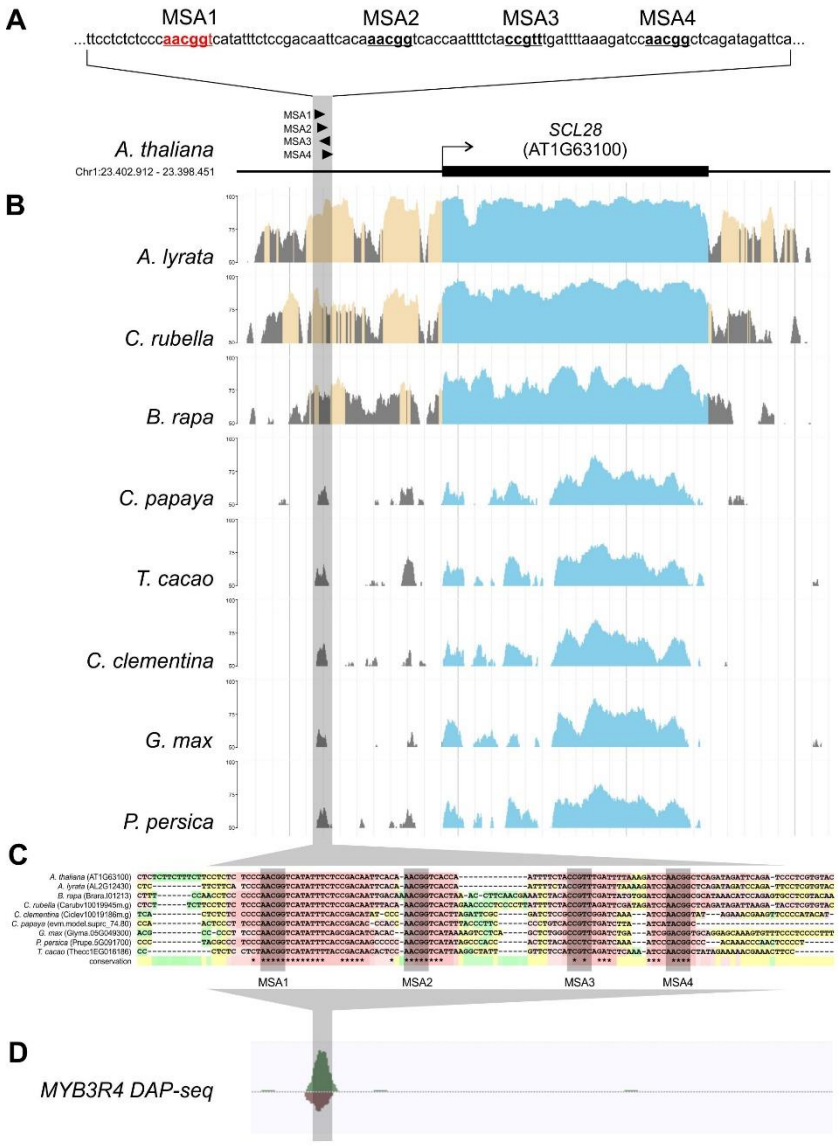

Figure S3. *Mitosis-specific activator* (*MSA*) elements in the *SCL28* promoter.
A. Schematic representation of *Arabidopsis thaliana SCL28 locus* indicating the four *MSA* elements found in the upstream regulatory regions. The core sequence of each *MSA* element is underlined and the *MSA* element deleted in the *ProSCL28ΔMSA1:SCL28 VENUS* construct is highlighted in red.
B and C. The *MSA* elements found in the *SCL28* promoter are conserved across plant species. **B.** VISTA plots obtained from the Phytozome V12.1 database with the whole genome alignments between *Arabidopsis thaliana* and other 8 species are shown. Nucleotides identities in 100 bp windows with values higher than 50% are plotted. **C.** Multiple sequence alignment of the conserved promoter region containing the *MSA* elements highlighted with gray boxes.
D. Experimental evidence for the binding of MYB3R4 to the *MSA* elements found in the promoter of *SCL28*. "MYB3R4 DAP-Seq" track shows the peaks retrieved from the Plant Cistrome Database derived from DAP-Seq experiments designed to detect *in-vitro* the binding sites of MYB3R4 to the *Arabidopsis thaliana* genome (O'Malley et al. (2016) Cell).

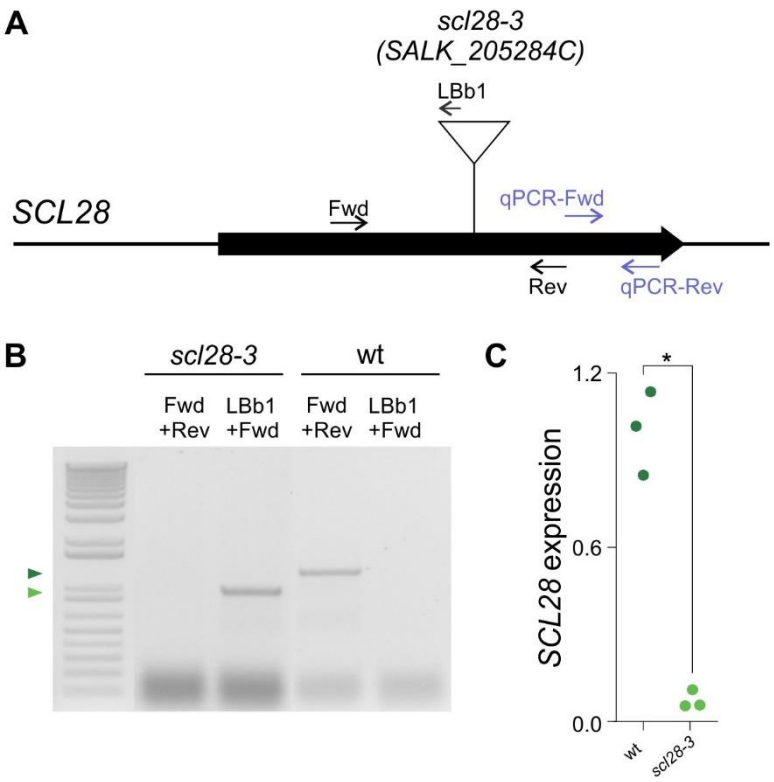

Figure S4. *scl28-3*, a mutant allele for SCL28.

A. Schematic representation of the *SCL28* locus indicating the T-DNA insertion in *scl28-3* (SALK_205284) and the oligonucleotide primers used for genotyping and RT-qPCR.

B. A representative agarose gel showing the amplification of the mutant (light-green arrowhead) and the wild-type (dark-green arrowhead) alleles of *SCL28* in wild-type and *scl28-3* plants.

C. Expression of *SCL28* in wild-type and *scl28-3.* Expression was estimated by RT-qPCR in three biological replicates and normalized to the mean value obtained in wild-type plants. Asterisks indicate significant differences (Student's t test, $p<0.05$).

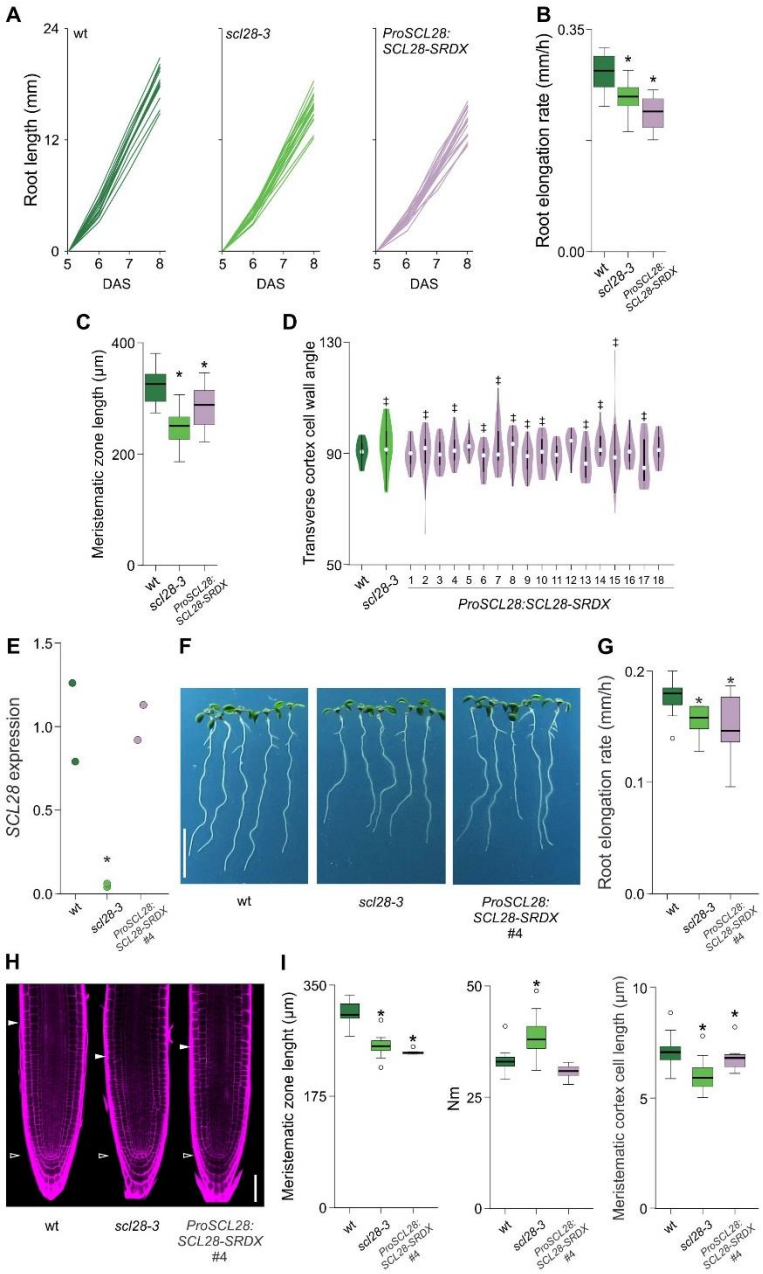

Figure S5. A dominant represor version of *SCL28* affects plant organ growth and meristem activity.
A. Distribution of root growth phenotypes in wild-type, *scl28-3* and in a population of 18 primary transgenic plants transformed with *ProSCL28:SCL28-SRDX*.
B. Root elongation rates (mm/h) calculated for each plant from panel A is shown as boxplots. Asterisks indicate significant differences with wild-type (Student´s t test, $p<0.05$).
C. Meristematic zone length (mm/h) of each plant from panel A is shown as boxplots. Asterisks indicate significant differences with wild-type (Student´s t test, $p<0.05$).
D. Combined box and violin plot diagrams of the angles between the transverse cortex cell wall and the main longitudnal axis of the root of 6 days-after-sowing *ProSCL28:SCL28-SRDX*. The data shown are the measurements of 40 cell walls from each plant. ‡ indicates significant differences in the variances (F test, $p<0.05$).

E. Expression of *SCL28* in wild-type, *scl28-3* and *ProSCL28:SCL28-SRDX* #4, a homozygous transgenic line selected for deeper characterization. Expression was estimated by RT-qPCR in 2 biological replicates and normalized to the mean value obtained in wild-type plants. Asterisks indicate significant differences from the wild-type (Student's t test, $p<0.05$).
F. Root phenotype in 10 days-old wild-type, *scl28-3* and *ProSCL28:SCL28-SRDX* plants. Scale bar = 1 cm.
G. Root elongation rate (mm/h) of wild-type, *scl28-3* and *ProSCL28:SCL28-SRDX* #4 plants. Boxplots with the measurements of 15 different plants of each genotype are shown. Asterisks indicate significant differences with wild-type (Student´s t test, $p<0.05$).
H. Root tip architecture in 6 days-after-sowing wild-type, *scl28-3* and *ProSCL28:SCL28-SRDX* #4 plants examined by LSCM in PI (magenta) stained plants. The white arrowheads mark the position of the QC and the end of the meristem where cells start to elongate. Scale bar = 50 µm.
I. Meristematic zone length, number of meristematic cortex cells (Nm) and length of meristematic cortex cells in the root meristem of wild-type, *scl28-3* and *ProSCL28:SCL28-SDRX* #4 plants. Boxplots with the measurements of 15 roots of each genotype are shown. Asterisks indicate significant differences with wild-type plants (Student´s t test, $p<0.05$).

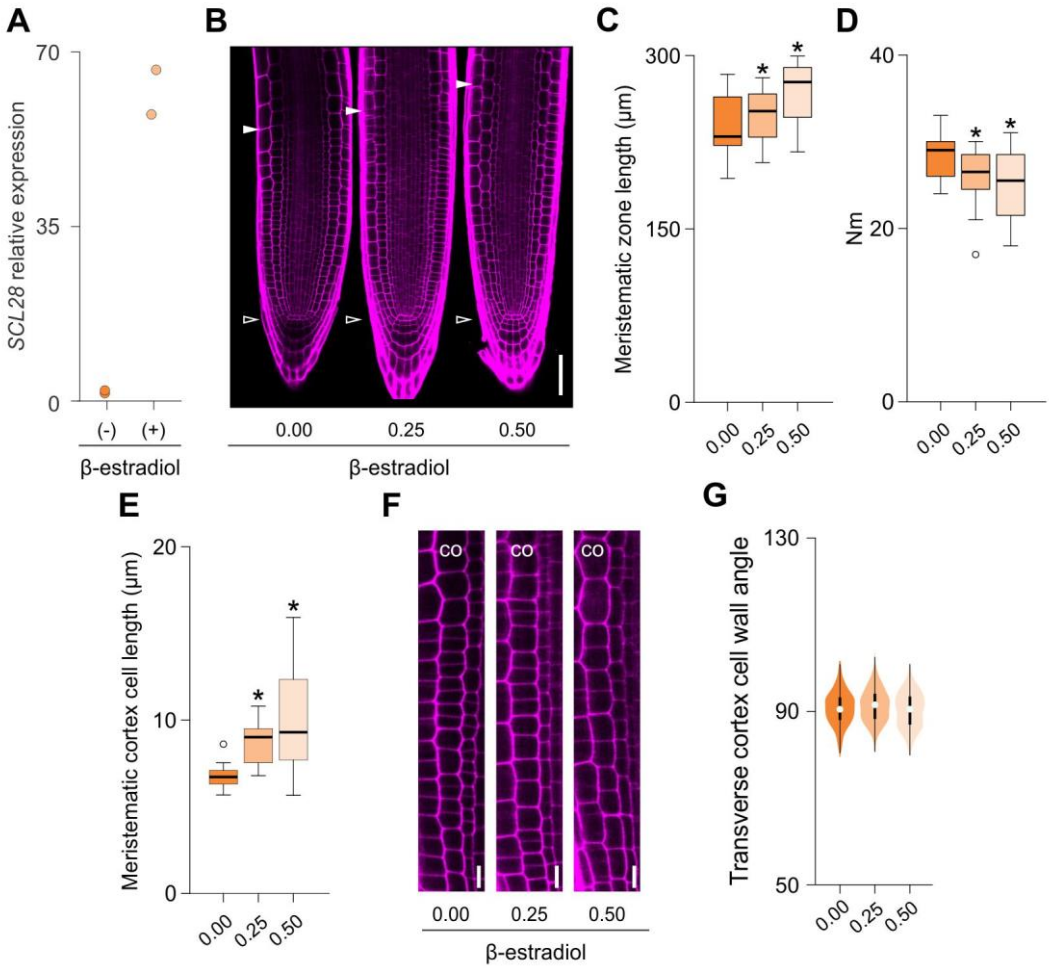

Figure S6. Overexpression of *SCL28* in a β-estradiol inducible line causes phenotypes opposite as those found in *scl28-3*.

A. Expression of *SCL28* in *XVE-SCL28* plants grown in media supplemented with 0.1 μM β–estradiol. Expression was estimated by RT-qPCR in two biological replicates and normalized to the mean value obtained in mock-treated control plants.

B. Root tip architecture of 6 days-after-sowing *XVE-SCL28* plants grown in media suplemented with 0.25 or 0.50 μM β-estradiol examined by LSCM in PI (magenta) stained plants. The white arrowheads mark the position of the QC and the end of the meristem where cells start to elongate. Scale bar = 50 μm.

C-E. Meristematic zone length (C), number of meristematic cortex cells (Nm) (D) and length of meristematic cortex cells (E) in the root meristem of *XVE-SCL28* plants grown in media suplemented with 0.25 or 0.50 μM β-estradiol. Boxplots with the measurements of 12 roots of each genotype are shown. Asterisks indicate significant differences with mock-treated plants (Student´s t test, $p<0.05$).

F. Detailed view of a file of meristematic cortex cells in *XVE-SCL28* plants grown in media supplemented with 0.25 or 0.50 μM β-estradiol. The label "co" indicates the file of meristematic cortex cells. Scale bar = 10 μm.

G. Combined box and violin plot diagrams of the angles between the transverse cortex cell wall and the main longitudnal axis of the root of 6 days-after-sowing *XVE-SCL28* plants grown in media suplemented with 0.25 or 0.50 μM β-estradiol. The data shown are the measurements of 20 cells in 12 different roots from each condition.

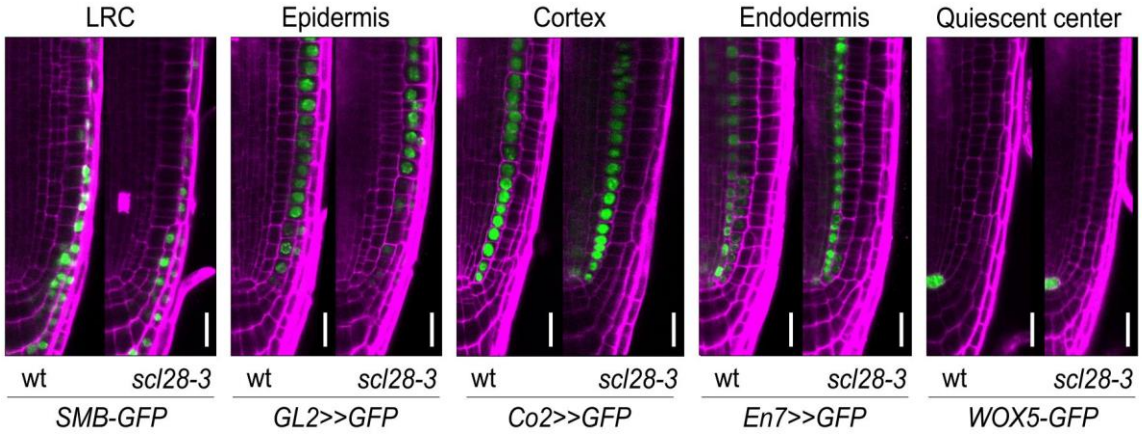

Figure S7. Cell patterning in *scl28-3* root.
Cell patterning in wild-type and *scl28-3* plants was evaluated by LSCM in PI (magenta) stained plants expressing reporters specific for lateral root cap (*SMB-GFP*), epidermis (*GL2>>GFP*), cortex (*Co2>>GFP*), endodermis (En7>>GFP) or the quiescent center (*WOX5-GFP*). In all cases, the fluorescence of the GFP reporter is shown in green.

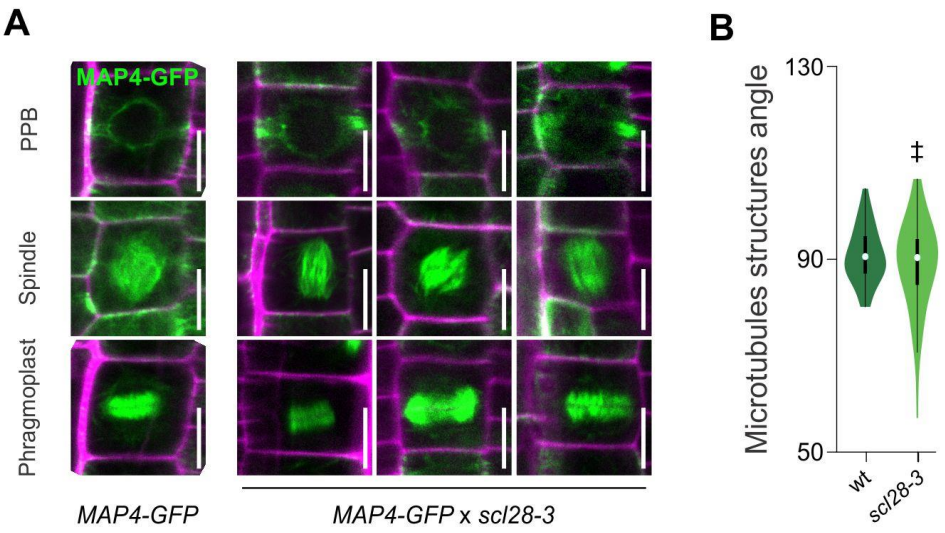

Figure S8. SCL28 modulates cell division plane orientation and cell wall biogenesis.
A. Microtubule arrays (pre-prophase band (PPB), mitotic spindle and phragmoplast) in meristematic cortex cells of wild-type and *scl28-3* plants. Microtubules are detected thanks to the *MAP4-GFP* reporter. Cell walls were stained with PI (magenta). Scale bar = 10 µm.
B. Combined box and violin plot diagram of the angles between the microtubule arrays (pre-prophase band (PPB), mitotic spindle and phragmoplast) and the main longitudnal axis of the root. The data shown are the measurements of 20 cells in 15 different roots of each genotype. ‡ indicates significant differences in the variances (F-test, $p<0.05$).

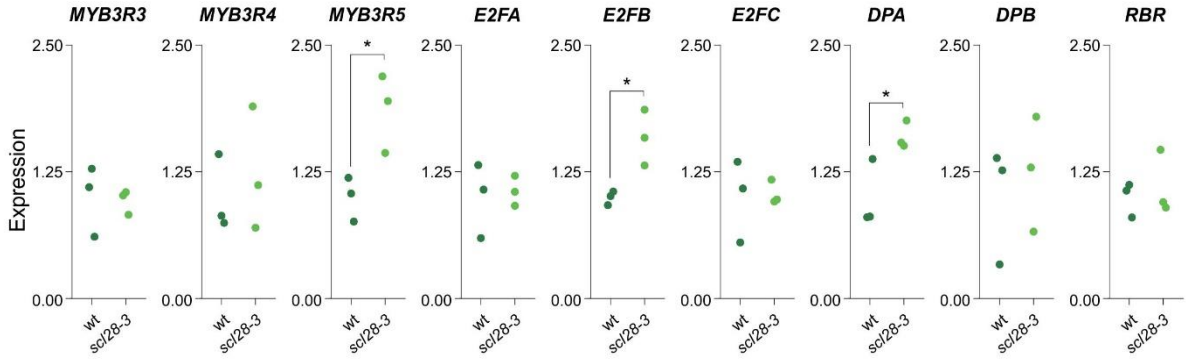

Figure S9. Expression of cell cycle regulators in wild-type and *scl28-3* plants.
Expression was estimated by RT-qPCR in three biological replicates and normalized to the mean value obtained in wild-type plants. Asterisks indicate significant differences (Student's t test, $p<0.05$).

Supplementary Tables

Table S1. Mutants and reporter lines used in this study.

Line	Line Description	Reference
scl28-3	Insertional mutant. SALK_205284	This work
myb3r3-1	Insertional mutant. SALK_041111C	Kobayashi *et al.* (2015) EMBO J.
myb3r4-1	Insertional mutant. SALK_059819C	Haga *et al.* (2007) Development
CYCB1;1-GFP	Mitotic Cyclin *CYCB1;1* reporter	Ubeda-Tomas *et al.* (2009) Curr Biol
SMB-GFP	Lateral Root Cap specific marker	Fendrych *et al.* (2014) Curr Biol
GL2>>GFP	Epidermis specific marker	Dietrich *et al.* (2017) Nature Plants
Co2>>GFP	Cortex specific marker	Dietrich *et al.* (2017) Nature Plants
En7>>GFP	Endodermis specific marker	Dietrich *et al.* (2017) Nature Plants
WOX5-GFP	Quiescent center specific marker	Sarkar *et al.* (2007) Nature
TUA2-RFP	Alpha tubulin 2 RFP reporter	Van Damme *et al.* (2004) Plant Phys
MAP4-GFP	Microtubules reporter	Marck *et al.* (1998) The Plant Cell
XVE-SCL28	β-estradiol *SCL28* inducible line	Coego *et al.* (2014) The plant Journal

Table S2. Binary plasmids generated in this study.

Vector	Construct	Arabidopsis Chromosome: Start-End
CG11	*ProSCL28:SCL28-VENUS*	[*ProSCL28:SCL28*, 1: 23402654 - 23399391] – *VENUS* CDS
CG22	*ProSCL28ΔMSA1:SCL28-VENUS*	[*ProSCL28ΔMSE*:*SCL28*, 1:23402654 - 23399391] [a] – *VENUS* CDS
CG18	*ProSCL28:SCL28-SRDX*	[*ProSCL28:SCL28*, 1: 23402654 - 23399391] – SRDX [b]
CG07	*Pro35S:SCL28*	*Pro35S:*[*SCL28*, Chr1:23401367 – 23399391]

[a] Coordinates of the deleted MSA: Chromosome 1, nucleotides 23402262-2340225.
[b] SRDX: Transcriptional repressor motif LDLDLELRLGFA (Hiratsu et al. (2003) The Plant Journal).
All constructs were cloned in the binary vector pCHF3 (Jarvis, P., Chen, L. J., Li, H., Peto, C. A., Fankhauser, C., and Chory, J. (1998). An Arabidopsis mutant defective in the plastid general protein import apparatus. Science 282, 100103). T-DNA constructs were introduced into *A. tumefaciens* strain ASE (Fraley, R. T., Rogers, S. G., Horsch, R. B., Eichholtz, D. A., Flick, J. S., Fink, C. L., Hoffmann, N. L., and Sanders, P. R. (1985) The SEV system: a new disarmed Ti plasmid vector system for plant transformation. Biotechnology 3, 629635).

Table S3. Oligonucleotide primers used in this study.

Gene	Locus ID	Sequence	Porpouse
SCL28	AT1G63100	GATGAAGACAACGGCGGTGAAG	RT-qPCR Forward primer
		TTCCCTCCGGTAGTCCAAGC	RT-qPCR Reverse primer
		GAAAGGACCACCGGAAACATC	Genotyping, Fwd [a]
		CCGTACATCCTAAGCAACATCT	Genotyping, Rev [a]
CYCB1;2	AT5G06150	TCCCTCCATGCTTGCTGCTTC	RT-qPCR Forward primer
		CCTGCTCTCACCGCATCTC	RT-qPCR Reverse primer
HISTONE H4	AT2G28740	ACCAAATTGCGTGTTTCCATTG	RT-qPCR Forward primer
		ATGTCTGGTCGTGGAAAGGGAG	RT-qPCR Reverse primer
MYB3R3	AT3G09370	TGATCAAAAGGTGAATGATGGT	RT-qPCR Forward primer
		TTCATCATCAGCTTTCTCTTCC	RT-qPCR Reverse primer
MYB3R4	AT5G11510	TGCCTGGAAGGTCGGATAATGGAA	RT-qPCR Forward primer
		CTGATCCAAAAGGCCAGACGACAT	RT-qPCR Reverse primer
MYB3R5	AT5G02320	TGGTAAGGACTTGGCGATGACAGA	RT-qPCR Forward primer
		GGACCTTGGACTCAAGAGGAGGAT	RT-qPCR Reverse primer
E2FA	AT2G36010	CAACCCAGAAACTGCTATTGT	RT-qPCR Forward primer
		GTCCGACTCATCATTTTCAAC	RT-qPCR Reverse primer
E2FB	AT5G22220	CCGATGAAAGAGGAAAGCACCG	RT-qPCR Forward primer
		CGCCTACCTCTGATCGAAACC	RT-qPCR Reverse primer
E2FC	AT1G47870	TGCCGTTATGACAGTTCTTTAGGG	RT-qPCR Forward primer
		AGTGTTCCATCCTCAGCTTCCT	RT-qPCR Reverse primer
DPA	AT5G02470	CTCGACTTCAATAGCACACCTTT	RT-qPCR Forward primer
		TGAGCGGAGCTATGTTGAGA	RT-qPCR Reverse primer
DPB	AT5G03415	TTTGATTTCAACAGCACTCCA	RT-qPCR Forward primer
		GCGTGAAATTGTGACAAAC	RT-qPCR Reverse primer
RBR	AT3G12280	GATCAAAGATGGATGCTC	RT-qPCR Forward primer
		TACAGATGCTATAACTGAAGA	RT-qPCR Reverse primer
RPS26C	AT3G56340	GACTTTCAAGCGCAGGAATGGTG	RT-qPCR Forward primer
		CCTTGTCCTTGGGGCAACACTTT	RT-qPCR Reverse primer
PP2A	AT1G13320	CCTGCGGTAATAACTGCATCT	RT-qPCR Forward primer
		CTTCACTTAGCTCCACCAAGCA	RT-qPCR Reverse primer

[a] To genotype for the T-DNA insertions, the LBb1 primer (GCGTGGACCGCTTGCTGCAACT) was used.

Supplementary Datasets (Separated files)

Dataset 1. Expression of CDKs and CYC in G2/M cells.

Dataset 2. Expression of Mitosis Specific Genes (MSG) in G2/M cells.

Dataset 3. Differentially expressed genes in G2/M cells when compared to whole meristems.

Dataset 4. Differentially expressed genes in G2/M cells when compared to whole meristems with expression enriched in the root meristem.

Dataset 5. Transcription factors enriched in G2/M cells.